PRESSURE DISTRIBUTION IN GAS MICROBEARING MODELED WITH FRACTIONAL DERIVATIVES FOR ALL RAREFACTION DEGREES

Nevena D. STEVANOVIĆ*, Snezana S. MILIĆEV

Faculty of Mechanical Engineering, University of Belgrade, Kraljice Marije 16, 11120 Belgrade, Serbia

*Corresponding author. *E-mail address:* nstevanovic@mas.bg.ac.rs

E-mail address: smilicev@mas.bg.ac.rs

Abstract

Velocity slip boundary condition for all Knudsen number values in microbearing gas flow is modeled by fractional derivative. For this purpose, a variant of Caputo derivative with the variable order α which depends on the local value of Knudsen number is applied. Such a universal boundary condition is implemented in the solving procedures of continuity and momentum equations, which leads to the general corrected Reynolds lubrication equation for all rarefaction degrees. An appropriate transformation of the variables enabled obtaining an analytical solution for mass flow rate and pressure distribution in the microbearing. The presented solution is in an excellent agreement with the solutions based on the kinetic theory for all regimes: continuum, slip, transition, and free molecular flow.

Keywords: slider microbearing, Reynolds lubrication equation, fractional derivative, Knudsen number, analytical solution.

1. Introduction

Gas flow in slider microbearings deviate from the continuum condition even at the atmospheric pressure. The level of deviation from the continuum, i.e. the level of rarefaction is estimated by the Knudsen number value, which is defined as the ratio of the mean free path of the molecules and the characteristic length. A gas flow is commonly classified according to the rarefaction as: continuum ($Kn<0.01$), slip ($0.01< Kn < 0.1$), transition ($0.1< Kn < 10$), or free-molecular flow regime ($Kn > 10$). Solutions for the slip flow regime are usually obtained by continuum equations with slip and temperature jump boundary conditions at the wall, while for the transition and free-molecular flow regimes the continuum approach breaks down. Generally, for modeling of a gas flow in the transition regime, an extended continuum equation with a range of various modified boundary conditions have been used, along with the direct simulation Monte Carlo (DSMC). Free-molecular flow obeys the laws of kinetic gas theory and has been solved numerically by the microscopic approach.

Deriving from the continuity and Navier-Stokes equations, together with the no-slip boundary condition, the classical compressible Reynolds lubrication equation determines the pressure generated in the bearing. In order to expand its application on the rarefied gas flow in microbearings, several Reynolds lubrication equations for the slip boundary conditions have been derived so far. This allows a simpler way for obtaining solutions, instead of solving the kinetic theory equations.

Burgdorfer [1] revises a Reynolds lubrication equation with the Maxwells first-order slip conditions at the wall. Mitsuya [2] used a 1.5-order slip boundary condition, while Hsia and Domoto [3] set up the second-order boundary condition model. These conditions, included in the continuity and momentum equations, lead to the 1.5-order and second-order Reynolds lubrication model, respectively. Lockerby et al. [4] and Barbar and Emerson [5] presented the reviews of the second-order boundary conditions that are appropriate for slip and early transition rarefaction regimes. Different slip models, which predicted different slip conditions at the slider surfaces were cited by Chen and Bogy [6]. Bahukudumbi and Beskok [7] derived a semi-analytical model for gas lubricated microbearings for a wide range of Knudsen number (Kn<12) using a modification of the viscosity coefficient by the rarefaction correction parameter. Sun et al. [8] obtained a modified Reynolds equation which could be applied regardless of the rarefaction degree by defining expressions for the effective viscosity, effective mean free path, and effective Knudsen number.

A way of extending the application of the continuum equations on the slip and transition flows is to apply the moment approximations derived from the Boltzmann equation, such as Grad's 13 moment equations (G13) [8] and the set of regularized 13 moment equations (R13) [9]. Also, a set of wall boundary conditions for the 13 moment equations based on the Maxwell wall-boundary model are derived by Gu and Emerson [10], which were later improved by Torrilhon and Struchtrup [11] and Gu and Emerson [12]. According to these extended continuum equations and boundary conditions defined from the regularized 13 moment equations, a modified Reynolds equation for the microbearing gas flow was established by Yang et al. [13]. Moreover, a Reynolds equation for slider microbearing gas flow also based on the R13 equations is derived from the kinetic theory by Gu et al. [14].

Furthermore, for the study of gas flow in transitional regime, the direct simulation Monte Carlo has been exploited by Alexander et al. [15], Liu and Ng [16], and John and Damodaran [17]. DSMC achieves reliable and accurate results, but it is computationally quite demanding.

Fukui and Kaneko [18,19] obtained a solution for the slider bearings for the entire Knudsen number range based on the linearized Boltzmann equation and Bhatnager–Gross–Krook (BGK) approach. This solution is used for checking other models for microbearing gas flow, but the process of getting results requires significant effort.

All previously mentioned Reynolds lubrication equations are finally solved numerically. Stevanovic and Djordjevic [20,21] obtained the analytical solution for the extended Reynolds lubrication equation based on second-order boundary conditions. That solution is appropriate for slip and early transition flow regimes.

In this paper, the slip boundary conditions for all Knudsen number values are defined by applying the fractional derivative. Using these slip boundary conditions together with continuity and Navier-Stokes equations, a new corrected Reynolds lubrication equation for all rarefaction degrees is obtained. It is solved analytically according to the approach previously presented [20,21] and the new solution holds for the entire Knudsen number range.

2. Problem description and mathematical formulation

In this paper a steady isothermal compressible gas flow in slider microbearing is analyzed (Fig. 1). The bottom plate is moving in the x direction with velocity u_w, while the upper plate is stationary. It is assumed that the distance between plates $h(x)$ is slowly varying, thus all variables also change very slowly in the x direction. Correspondingly, the velocity component in the y direction is much smaller than the stream-wise component. Moreover, the gas flow is slow, with low Mach number, so the inertia effect is neglected. Based on these assumptions, the continuity and momentum equations could be simplified [22]:

$$\dot{M} = \frac{1}{RT}\int_0^h pu\mathrm{d}y = const \,, \tag{1}$$

$$\frac{\mathrm{d}p}{\mathrm{d}x} = \mu\frac{\partial^2 u}{\partial y^2}\,, \tag{2}$$

$$\frac{\partial p}{\partial y} = 0\,, \tag{3}$$

$$\frac{p}{\rho} = \mathrm{R}T\,, \tag{4}$$

where x, y, p, ρ, T, R, u and $\dot{M}$ are stream-wise and cross-wise coordinates, pressure, density, temperature, gas constant, velocity component in the x direction and the mass flow rate per unit width, respectively. Since the flow is isothermal, it is assumed that the dynamic viscosity μ is constant.

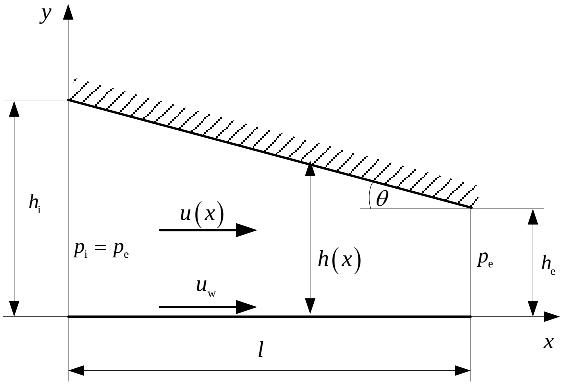

Fig. 1. Schematic view of microbearing

The fractional calculus has proven to be a useful mathematical tool and a natural framework for many phenomena. Thus, the fractional derivative in Caputo sense is applied for modelling the partial differential equations that enables solving problems in different fields: diffusion or dispersion problems [23], heat transfer problems [24], for analyzing rheological properties of cells [25], etc. In this paper, the gas velocity is modeled at the wall with a fractional derivative, in order to expand the application of the continuum theory to the entire Knudsen number range. We use a form of Caputo derivative [26]:

$$ {}_{y}C_{\lambda}^{(\alpha)}(u) = \int_y^{\lambda(x)} \left.\frac{\partial u}{\partial y}\right|_{y=\eta} (\eta - y)^{-\alpha(x)}\,\mathrm{d}\eta \tag{5}$$

with $0 \le y \le \lambda(x)$ and $0 \le \alpha(x) < 1$, where λ is the local value of the mean free path of molecules and $\alpha(x)$ is the variable order of the derivative. Hence, the slip velocities at the bottom and top walls are modelled as:

$$y=0: \qquad u=u_0(x)=u_{\mathrm{w}}+\frac{2-\sigma_v}{\sigma_v}h(x)^{\alpha(x)}\int_0^{\lambda(x)}\left.\frac{\partial u}{\partial y}\right|_{y=\eta}(\eta)^{-\alpha(x)}\,d\eta\,, \tag{6}$$

$$y=h(x): \qquad u=u_1(x)=\frac{2-\sigma_v}{\sigma_v}h(x)^{\alpha(x)}\int_0^{\lambda(x)}\left.\frac{\partial u}{\partial \tilde{y}}\right|_{\tilde{y}=\eta}(\eta)^{-\alpha(x)}\,d\eta\,, \tag{7}$$

where $\tilde{y}=h(x)-y$, σ_v is the tangential momentum accommodation coefficient, while $u_0(x)$ and $u_1(x)$ are the gas slip velocities at the lower and upper plates.

The molecular mean-free path $\lambda=\mu\sqrt{\pi RT/2}\big/p$ for isothermal flow depends on pressure, i.e. according to Equation (3), only on the coordinate x. That is why the local Knudsen number $\mathrm{Kn}(x)=\lambda(x)/h(x)$ depends on x only. Hence, the order of the derivative $\alpha(x)$ could be expressed via the local value of Knudsen number, $\alpha(\mathrm{Kn})$. Moreover, ~~α~~ α =0 for the continuum flow regime (Kn=0), while $\alpha \to 1$ for the free molecular flow ($\mathrm{Kn} \to \infty$). From now on, $\lambda(x)$, $\mathrm{Kn}(x)$, $h(x)$, $u(x)$, $u_0(x)$, $u_1(x)$, $p(x)$, and $\alpha(\mathrm{Kn})$ will be denoted as λ, Kn, h, u, u_0, u_1, p, and α, respectively.

The momentum equation (2) and boundary conditions (6) and (7) lead to the solution for the velocity field in the slider microbearing:

$$u=\frac{y^2}{2\mu}\frac{\mathrm{d}p}{\mathrm{d}x}-\left(\frac{h^2}{2\mu}\frac{\mathrm{d}p}{\mathrm{d}x}+u_0-u_1\right)\frac{y}{h}+u_0\,. \tag{8}$$

According to this solution for velocity, boundary conditions (6) and (7) become:

$$y=0: \qquad u=u_0=u_{\mathrm{w}}\frac{1+K_1}{1+2K_1}+\frac{h^2}{2\mu}\frac{\mathrm{d}p}{\mathrm{d}x}\left(2K_2-K_1\right), \tag{9}$$

$$y=h: \qquad u=u_1=u_0-\frac{u_{\mathrm{w}}}{1+2K_1}\,, \tag{10}$$

where K_1 and K_2 depend on Knudsen number, $K_1=\dfrac{2-\sigma_v}{\sigma_v}\dfrac{\mathrm{Kn}^{1-\alpha}}{1-\alpha}$ and $K_2=\dfrac{2-\sigma_v}{\sigma_v}\dfrac{\mathrm{Kn}^{2-\alpha}}{2-\alpha}$.

By applying the solution for the stream-vice velocity (8) to the continuity equation (1), where the variable gas density is expressed by the equation of state (4), the differential equation for the pressure along the microbearing is obtained:

$$\dot{M}=-\frac{1}{12\mu\mathrm{R}T}\frac{\mathrm{d}p}{\mathrm{d}x}h^3p+\frac{u_0+u_1}{2\mathrm{R}T}hp\,. \tag{11}$$

Equation (11) in the non-dimensional form is:

$$m=-\frac{1}{\Lambda}\frac{\mathrm{d}P}{\mathrm{d}X}H^3P+\left(U_0+U_1\right)HP\,, \tag{12}$$

where X, H, P, U_0 and U_1 are non-dimensional stream-wise coordinate, height, pressure and slip velocities at the walls, scaled by microbearing length l, the microbearing height at the exit h_{e}, the pressure at the microbearing exit p_{e} and the velocity of the lower bearing wall u_{w}, respectively. Moreover, in the non-dimensional equation (12) two non-dimensional parameters appear: the bearing number $\Lambda=\dfrac{6\mu u_{\mathrm{w}}l}{p_{\mathrm{e}}h_{\mathrm{e}}^2}$ and parameter $m=\dot{M}\big/\dot{M}_{\mathrm{C}}$, where $\dot{M}_{\mathrm{C}}=\dfrac{p_{\mathrm{e}}h_{\mathrm{e}}u_{\mathrm{w}}}{2\mathrm{R}T}$ is the Couette mass flow rate for continuum expressed by the gas flow properties at the bearing exit. For a microbearing whose cross section changes linearly (Fig. 1), its dimensionless height is defined as $H=H_{\mathrm{i}}-(H_{\mathrm{i}}-1)X$, where $H_{\mathrm{i}}=h_{\mathrm{i}}/h_{\mathrm{e}}$ is the dimensionless inlet microbearing height.

The dimensionless gas velocities at the walls U_0 and U_1 and their sum U_0+U_1 follow from the dimensional forms (9) and (10):

$$U_0 = \frac{1+K_1}{1+2K_1} + \frac{3H^2}{\Lambda}\frac{\mathrm{d}P}{\mathrm{d}X}\left(2K_2 - K_1\right), \tag{13}$$

$$U_1 = U_0 - \frac{1}{1+2K_1}, \tag{14}$$

$$U_0 + U_1 = 1 - \frac{6}{\Lambda}H^2\frac{\mathrm{d}P}{\mathrm{d}X}\left(K_1 - 2K_2\right). \tag{15}$$

Now, Equation (12) finally gets the form of the general corrected Reynolds lubrication equation for the entire Knudsen number range:

$$m = \frac{-1}{\Lambda}\frac{\mathrm{d}P}{\mathrm{d}X}\left[1+6\left(K_1-2K_2\right)\right]H^3P + HP. \tag{16}$$

For continuum flow conditions, i.e. for Kn = 0, as expected, Equations (16) naturally come down to the classical form of the Reynolds lubrication equation for the no-slip compressible flow in the bearing.

Since the molecular mean-free path is inversely proportional to the pressure, the correlation between local Knudsen number ($\mathrm{Kn} = \lambda / h$) and reference Knudsen number ($\mathrm{Kn_e} = \lambda_e / h_e$) for isothermal gas flow in microbearing is:

$$\frac{\mathrm{Kn}}{\mathrm{Kn_e}} = \frac{1}{HP}. \tag{17}$$

In order to obtain the analytical solution, we transform differential equation (16) using correlation between pressure and Knudsen number (17):

$$m = \frac{\mathrm{Kn_e^2}}{\Lambda \mathrm{Kn}^2}\left[1+6\left(K_1-2K_2\right)\right]\left(1 - H_\mathrm{i} + \frac{H}{\mathrm{Kn}}\frac{\mathrm{dKn}}{\mathrm{d}X}\right) + \frac{\mathrm{Kn_e}}{\mathrm{Kn}}, \tag{18}$$

where $F(\mathrm{Kn}) = 6\left(K_1 - 2K_2\right)$. Values of the Knudsen number at the microbearing inlet and exit are defined by the following boundary conditions:

$$X = 0: \quad H = H_\mathrm{i}, P = 1 \Rightarrow \mathrm{Kn} = \mathrm{Kn_e}/H_\mathrm{i}, \tag{19}$$

$$X = 1: \quad H = 1, P = 1 \Rightarrow \mathrm{Kn} = \mathrm{Kn_e}. \tag{20}$$

Separation of variables Kn and X in equation (18) gives the separable differential equation:

$$\frac{\mathrm{d}X}{H_\mathrm{i} - \left(H_\mathrm{i}-1\right)X} = \frac{\mathrm{Kn_e^2}\left[1+F(\mathrm{Kn})\right]\mathrm{dKn}}{\Lambda m \mathrm{Kn}^3 - \Lambda \mathrm{Kn_e}\mathrm{Kn}^2 + \left(H_\mathrm{i}-1\right)\left[1+F(\mathrm{Kn})\right]\mathrm{Kn_e^2}\mathrm{Kn}}, \tag{21}$$

which solution can be obtained by quadrature. The integral of Equation (21) from the inlet to the outlet cross-section, by applying the boundary conditions (19, 20)

$$\frac{\ln H_\mathrm{i}}{H_\mathrm{i}-1} = \int_{\mathrm{Kn_e}/H_\mathrm{i}}^{\mathrm{Kn_e}} \frac{\mathrm{Kn_e^2}\left[1+F(k)\right]\mathrm{d}k}{\Lambda m k^3 - \Lambda \mathrm{Kn_e} k^2 + \left(H_\mathrm{i}-1\right)\left[1+F(k)\right]\mathrm{Kn_e^2}k} \tag{22}$$

enables obtaining the value of the parameter m. Here k is dummy variable. To calculate the value of the parameter m, apart from three non-dimensional parameters (H_i, Λ and $\mathrm{Kn_e}$) that define a gas flow in microbearing, the function F(Kn) should be defined also. In order to determine F(Kn), it is necessary to know the correlation between the Knudsen number and the order of the derivative α. By comparing the generalized Reynolds lubrication equation (16) with the corresponding one based on the Boltzmann equation [18], it follows:

$$\tilde{Q}_p = 1 + 6\left(K_1 - 2K_2\right), \text{ i.e. } \tilde{Q}_p = 1 + F(\mathrm{Kn}). \tag{23}$$

Here $\tilde{Q}_p$ is the normalised flow rate coefficient of Poiseuille flow. We defined the values of $\tilde{Q}_p$ for the specified Knudsen numbers by applying the numerical solution of the Boltzmann equation presented by the power series expressions with errors less than 1% [19]. For so determined $\tilde{Q}_p$ for certain Knudsen number values, α is found from Equation (23). Moreover, we created by fitting the analytical relations between α and Kn for the three Knudsen number domains:

$$\mathrm{Kn} \le 0.1, \quad \alpha = -\frac{0.096207}{\xi} - \frac{0.253681}{\xi^2} - \frac{0.44223}{\xi^3} - \frac{0.188534}{\xi^4}, \tag{24}$$

$$0.1 < \mathrm{Kn} \le 10, \quad \alpha = 0.462839\,\mathrm{Tanh}\left[1.86821(\xi + 0.184743)\right] + 0.518343, \tag{25}$$

$$\mathrm{Kn} > 10, \quad \alpha = 1 - \frac{0.00999168}{\xi} + \frac{0.0697065}{\xi^2} - \frac{0.145592}{\xi^3} + \frac{0.061911}{\xi^4}, \tag{26}$$

where $\xi = \log_{10}\mathrm{Kn}$.

Now, for certain H_i, Λ, $\mathrm{Kn_e}$, and appropriate relation between α and Kn, the parameter m can be found from Equation (22) numerically. After calculating the parameter m, the Knudsen number distribution can be obtained by integrating Equation (21) from arbitrary to the outlet cross section of the microbearing:

$$\frac{\ln\left[H_\mathrm{i} - (H_\mathrm{i} - 1)X\right]}{1 - H_\mathrm{i}} = \int_{\mathrm{Kn}}^{\mathrm{Kn_e}} \frac{\mathrm{Kn_e^2}\left[1 + F(k)\right]\mathrm{d}k}{\Lambda m k^3 - \Lambda \mathrm{Kn_e} k^2 + (H_\mathrm{i} - 1)\left[1 + F(k)\right]\mathrm{Kn_e^2} k}. \tag{27}$$

Finally, the pressure distribution along the microbearing follows from the Knudsen number distribution (27) and correlation (17).

3. Results and discussion

Solutions for the pressure distribution obtained from the general corrected Reynolds lubrication equation presented in this paper are compared with the numerical solution of the Boltzmann equation proposed by Fukui and Kaneko [18]. Fig. 2 and Fig. 3 show those results for the dimensionless inlet height of microbearing $H_\mathrm{i} = 2$ and tangential momentum accommodation coefficient $\sigma_v = 1$. Fig. 2 presents the pressure distribution for the bearing number Λ=1, while Fig. 3 corresponds to the bearing number Λ=10. Both figures comprise results for the whole Knudsen number range. In Figs. 2a and 3a) the diagrams present the results for the slip flow regime (Kn ≤ 0.1), in Figs. 2b and 3 b results for the transitional flow regime (0.1 < Kn ≤ 10), while in Figs. 2c and 3c the results correspond to the free molecular flow (Kn > 10). The results for the slip regime (Figs. 2a and 3a) are obtained using α dependence on Knudsen number defined by Equation (24), for the transition regime (Figs. 2b and 3b) results are obtained using α dependence on Knudsen number defined by Eq. (25) and for the free molecular flow (Figs. 2c and 3c) the results are obtained using α dependence on Knudsen number defined by Equation (26).

Higher values of Knudsen number (higher rarefaction) correspond to lower pressure along the microbearing and lower load carrying capacity. Moreover, the pressure in the microbearing and therefore load carrying capacity increase with the increase of the bearing number Λ.

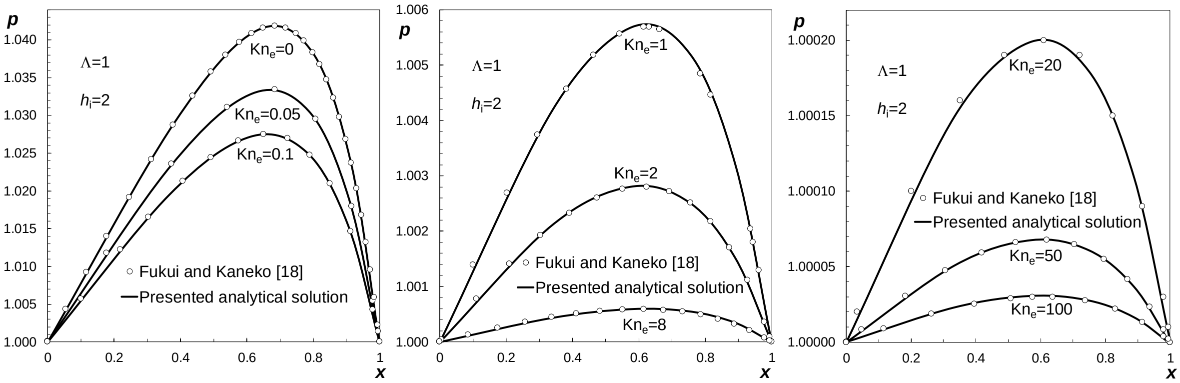

a) b) c)

Fig. 2 Pressure along the microbearing: the presented solution and the solution obtained by Boltzmann equation [18] for Λ = 1 and $H_i = 2$; a) Kn ≤ 0.1; b) 0.1 < Kn ≤ 10; c) Kn > 10.

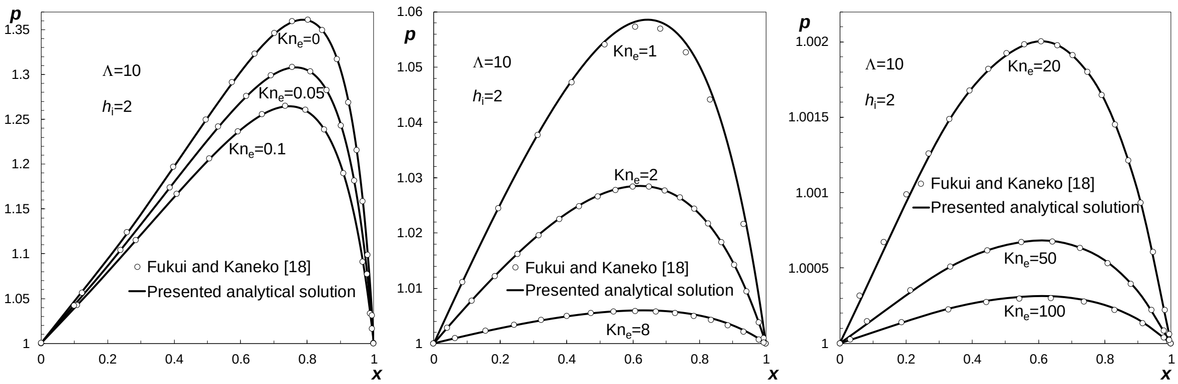

a) b) c)

Fig. 3 Pressure along the microbearing: the presented solution and the solution obtained by Boltzmann equation [18] for Λ = 10 and $H_i = 2$; a) Kn ≤ 0.1; b) 0.1 < Kn ≤ 10; c) Kn > 10.

Fig. 4 presents the pressure distributions for different ratios of the inlet and outlet microbearing heights H_i =1.2, 1.6, 2, and 2.6, i.e. different pitching angles θ_i =0.002, 0.006, 0.01, and 0.016 rad. It shows the comparison between the presented solution of the general corrected Reynolds lubrication equation for all Knudsen number values with the DSMC data obtained by Liu and Ng [16] and the results derived from the extended Reynolds equation based on regularized 13 moment equations obtained by Gu et al. The results correspond to the transition regime ($Kn_e = 1.24$) and bearing number Λ = 61.6. Our results reproduce the DSMC data of Liu and Ng [16] with good accuracy, even better than the results of Gu et al. [14] whose discrepancy from the DSMC data [16] is up to 1.5%. Moreover, Fig. 4 indicates that the position of the pressure maximum slightly moves towards the microbearing exit as the ratios of the inlet and outlet microbearing height H_i increases.

Fig. 5 shows the influence of the bearing number on the pressure in microbearing along with the comparison with the results of Gu et al. [14] and Alexander et al. [15]. The results are presented for the ratio of inlet and outlet microbearing heights $H_i = 2$, Knudsen number $Kn_e = 1.24$, and three values of bearing numbers Λ = 61.6, 123.2, and 221.8. The predicted pressure distribution from our model are in a very good agreement with both researches [14,15]. Moreover, Fig. 5 indicates that the position of the load center moves towards the microbearing exit with the increase of the bearing number.

The influence of the wall velocity on the pressure distribution in microbearing is presented in Fig. 6 for bearing length l = 0.1m, inlet height h_i = 66μm, exit height h_e = 10μm, ambient pressure p = 101325 Pa, ambient density ρ = 1.1853kg/m^3 and dynamic viscosity μ = 18.46 · 10^{-6} Pas. Our results agree very well with the numerical results obtained by Holey et al. [27].

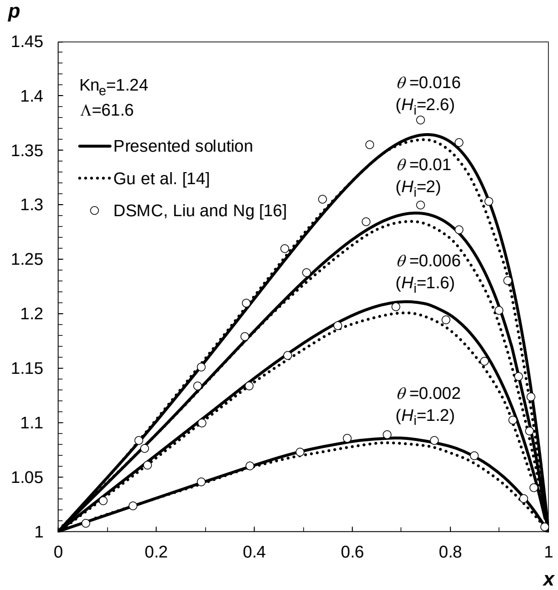

Fig. 4 Pressure distribution (the presented model, Gu et al. [14], and Liu and Ng [16]) for the reference Knudsen number $\mathrm{Kn_e}$ = 1.24 and the bearing number Λ=61.6 for different H_i =1.2, 1.6, 2, and 2.6 (pitching angles θ_i = 0.002, 0.006, 0.01, and 0.016 rad)

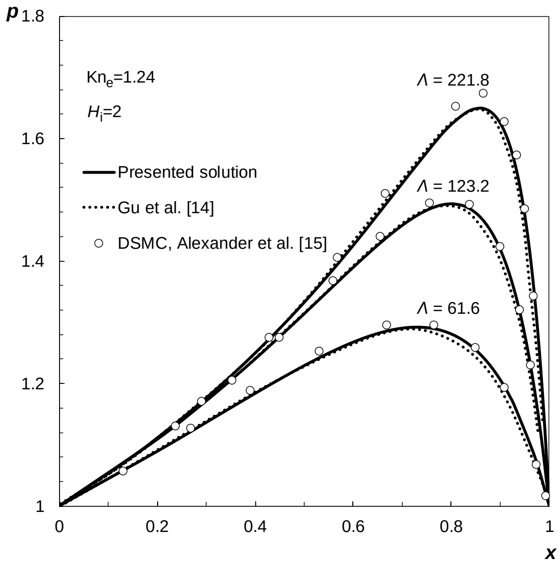

Fig. 5 Pressure distribution (the presented model, Gu et al. [14], and Alexander et al. [15]) for the reference Knudsen number $\mathrm{Kn_e}$ = 1.24 and H_i = 2 (pitching angle θ = 0.01) for different bearing numbers Λ=61.6, 123.2 and 221.8

4. Conclusion

A new analytical solution for the compressible isothermal two-dimensional and low Much number gas flows in slider microbearings for the whole range of Knudsen number has been presented. The ability of the obtained solution to cover the slip, transition, and free-molecular flow has been achieved by modeling velocity boundary conditions by a fractional derivative. It has been found that the order of the fractional derivative $\alpha(x)$ that varies along microbearing can be expressed as the function of the local Knudsen number value since it also changes only with the x axis value. That correlation between α and Knudsen number is found based on the values of the normalized flow rate coefficient of Poiseuille flow $\tilde{Q}_p$ for certain Knudsen number obtained from the numerical solution of the Boltzmann equation [19]. Three correlations among the order of the fractional derivative α and the local Knudsen number value, for three different Knudsen number ranges, are defined to achieve the best fit.

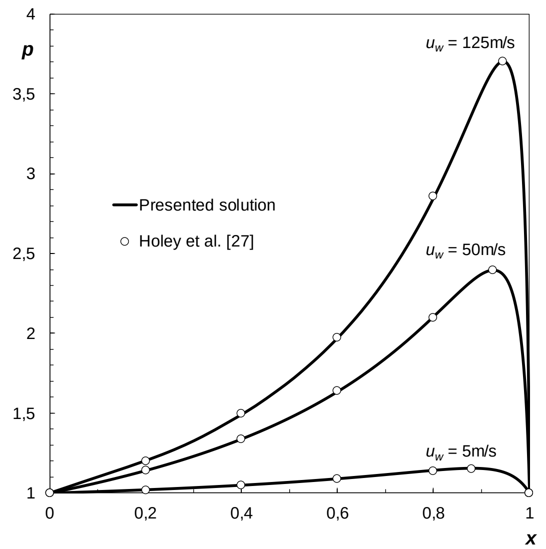

Fig. 6 Pressure distribution (the presented model, Holey et al. [27]) for different wall velocities u_w (5m/s, 50m/s, 125m/s)

Here obtained general corrected Reynolds lubrication equation for all rarefaction degrees was analytically solved. Expressing the local pressure via Knudsen number enabled separation of variables and obtaining the mass flow rate, the Knudsen number distribution, and finally, the pressure distribution along microbearing.

The presented solution for pressure in slider microbearings, based on the continuum equations and slip boundary conditions modeled by the fractional derivative, is much easier to obtain than a numerical solution of the Boltzmann equation and DSMC. Even though our solution follows from the continuum equations, a very good agreement with the Boltzmann equation and DSMC is achieved for all degrees of rarefaction. This comparative analysis has shown the reliability of the obtained analytical solution for pressure distribution in slider microbearings in the whole range of Knudsen numbers.

A similar approach could be applied for modeling the slip boundary conditions in microchannels and microtubes with slowly varying cross-section. In this way, it would be possible to obtain solutions for gas flow in those geometries, due to the pressure difference between the inlet and outlet, with the aim of including all levels of rarefaction with a macroscopic approach.

Acknowledgments

The authors would like to express their gratitude to the late Professor Vladan Đorđević for his inspiring and useful comments on early drafts of this paper. This work was supported by the Ministry of Education, Science and Technological Development, Republic of Serbia [contract number 451-03-47/2023-01/200105, February, 3rd2023].

Nomenclature

h - microbearing height, [m]
H - nondimensional microbearing height, [-]
l - microbearing length, [m]
Kn- local Knudsen number, [$=\lambda/h$], [-]
$\dot{M}$ - mass flow rate per unit width, [kgm^{-1}s^{-1}]
$\dot{M}_C$ - Couette mass flow rate per unit width for continuum expressed by the properties at the bearing exit, [$=p_e h_e u_w/2RT$], [kgm^{-1}s^{-1}]
m - parameter, [$=\dot{M}/\dot{M}_C$], [-]
$\tilde{Q}_p$ - normalised flow rate coefficient of Poiseuille flow, [-]
p- pressure, [Pa]
P - nondimensional pressure, [-]
R - gas constant, [Jkg^{-1}K^{-1}]
T - temperature, [K]
u - velocity component in the x direction, [ms^{-1}]
U - nondimensional velocity, [-]
x, y - coordinates, [m]
X - nondimensional coordinate, [-]
α - order of the derivative, [-]
λ - mean free path, [m]
Λ - bearing number[$=6\mu u_w l/p_e h_e^2$], [-]
μ - dynamic viscosity, [Pa s]
ρ - density, [kgm^{-3}]
σ_v - momentum accommodation coefficient, [-]
θ - pitching angle, [rad]

Indexes

e - exit parameter
i - inlet parameter
0 - parameters at the lower wall
1 - parameters at the upper wall

References

[1] Burgdorfer, A., The influence of the molecular mean free path on the performance of hydrodynamic gas lubricated bearing, *J. Basic Eng. Trans*., *81* (1959), pp. 94–100

[2] Mitsuya, Y., Modified Reynolds equation for ultra-thin film gas lubrication using 1.5-order slip-flow model and considering surface accommodation coefficient, *ASME J. Trib. 115*, (1993), pp. 289-294

[3] Hsia, Y., Domoto, G., An experimental investigation of molecular rarefaction effects in gas-lubricated bearings at ultra low clearances, *J. Lubr. Technol. 105* (1983), pp. 120-130

[4] Lockerby, D. A., *et al*., Velocity boundary condition at solid wall in rarefied gas calculation, *Phys. Rev. E 70*, 017303 (2004)

[5] Barber, R. E., Emerson, D. R., Challenges in modelling gas-phase flow in microchannels: from slip to transition, *Heat Transfer Eng. 27* (2006), pp. 3-12

[6] Chen, D., Bogy, D. B., Comparisons of Slip-Corrected Reynolds Lubrication Equations for the Air Bearing Film in the Head-Disk Interface of Hard Disk Drives, *Tribol. Lett. 37* (2010), pp. 191-201

[7] Bahukudumbi, P., Beskok, A., A Phenomenological lubrication model for the entire Knudsen Regime, *J. Micromech. Microeng. 13* (2003), 6, pp. 873-884

[8] Sun, Y.H., *et al*., A slip model for gas lubrication based on an effective viscosity concept, *J. Eng. Tribol. 217* (2003), pp. 187-195

[9] Struchtrup H., Torrilhon, M., Regularization of Grad's 13 moment equations: Derivation and linear analysis, *Phys. Fluids 15* (2003), 9, pp. 2668–2680

[10] Gu, X.J., Emerson, D.R., A computational strategy for the regularized 13 moment equations with enhanced wall-boundary conditions, *J. Comput. Phys. 225* (2007), 1, pp. 263-283

[11] Torrilhon, M., Struchtrup, H., Boundary conditions for regularized 13-moment-equations for micro-channel-flows, *J. Comput. Phys. 227* (2008), pp. 1982–2011

[12] Gu, X.J., Emerson, D.R., A high-order moment approach for capturing non-equilibrium phenomena in the transition regime, *J Fluid Mech. 636* (2009), pp. 177-216

[13] Yang, Q., *et al*., Improved modified Reynolds equation for thin-film gas lubrication from an extended slip velocity boundary condition, *Microsyst Technol. 22* (2016), pp. 2869-2875

[14] Gu, X.J., *et al*., A new extended Reynolds equation for gas bearing lubrication based on the method of moments, *Microfluidics and Nanofluidics 20*:*23* (2016)

[15] Alexander, F.J., *et al*., Direct simulation Monte Carlo for thin-film bearings, *Phys. Fluids*, *6* (1994), 12, pp. 3854-3860

[16] Liu, N., Ng, E.Y.K., The posture effects of a slider air bearing on its performance with a direct simulation Monte Carlo method, *J. Micromech. Microeng. 11* (2001), 5, pp. 463-473

[17] John, B., Damodaran, M., Computation of head–disk interface gap micro flowfields using DSMC and continuum–atomistic hybrid methods, *Int. J. Numer. Meth. Fluids, 61* (2009), pp. 1273–1298

[18] Fukui, S., Kaneko, R., Analysis of ultra-thin gas film lubrication based on linearized Boltzmann equation: First report-derivation of a generalized lubrication equation including thermal creep flow, *J. Tribol. 110* (1988), pp. 253-262

[19] Fukui, S., Kaneko, R., A database for interpolation of Poiseuille flow rates for high Knudsen number lubrication problems, *J. Tribol. 112* (1990), pp. 78-83

[20] Stevanovic, N. D., Djordjevic, V. D., The exact analytical solution for the gas lubricated bearing in the slip and continuum flow regime, *Publications de l'Institute mathematique 91* (2012), pp. 83-93

[21] Stevanovic, N. D., Djordjevic, V. D., An exact analytical solution for the second order slip-corrected Reynolds lubrication equation, *FME Transactions, 43* (2015), pp. 16-20

[22] Szeri, A. Z., *Fluid film lubrication: theory and design*, Cambridge University Press, Cambridge, 1998

[23] Aghdam, Y. E., et al., Numerical approach to simulate diffusion model of a fluid-flow in porous media, *Thermal Sciense*, *25* (2021), 2, pp. 251-261

[24] Gundogdu, H. and Gozukizil, O. F., On the approximate numerical solutions of fractional heat equation with heat source and heat loss, 26 (2022), 5, pp. (3773-3776)

[25] Djordjevic, V., *et al*., Fractional Derivatives Embody Essential Features of Cell Rheological Behavior, *Annals of Biomedical Engineering*, 31 (2003), pp. 692-699

[26] Podlubny, I., *Fractional Differential Equations*, Academic Press, 1999

[27] Holey, H., *et al*., Height‑Averaged Navier–Stokes Solver for Hydrodynamic Lubrication, *Tribol. Lett.*, 70:36 (2022)

Submitted: 14.4.2024.

Revised: 1.6.2024.

Accepted: 9.6.2024.